Broadband true time delay for microwave signal processing, using slow light based on stimulated Brillouin scattering in optical fibers

Sanghoon Chin,[1,*] Luc Thévenaz,[1] Juan Sancho,[2] Salvador Sales,[2] José Capmany,[2] Perrine Berger,[3] Jérôme Bourderionnet,[3] and Daniel Dolfi[3]

[1]*Ecole Polytechnique Fédérale de Lausanne, STI-GR-SCI-LT Station 11, CH-1015 Lausanne, Switzerland*
[2]*iTEAM Institute, Universidad Politécnica de Valencia, 46022 Valencia, Spain*
[3]*Thales Research & Technology, 1 av. Augustin Fresnel, 91767 Palaiseau Cedex, France*
**sanghoon.chin@epfl.ch*

Abstract: We experimentally demonstrate a novel technique to process broadband microwave signals, using all-optically tunable true time delay in optical fibers. The configuration to achieve true time delay basically consists of two main stages: photonic RF phase shifter and slow light, based on stimulated Brillouin scattering in fibers. Dispersion properties of fibers are controlled, separately at optical carrier frequency and in the vicinity of microwave signal bandwidth. This way time delay induced within the signal bandwidth can be manipulated to correctly act as true time delay with a proper phase compensation introduced to the optical carrier. We completely analyzed the generated true time delay as a promising solution to feed phased array antenna for radar systems and to develop dynamically reconfigurable microwave photonic filters.

©2010 Optical Society of America

OCIS codes: (060.2310) Fiber optics; (070.1170) Analogue signal processing; (290.5900) Scattering, stimulated Brillouin; (060.4370) Nonlinear optics, fibers.

References and links

1. J. Capmany, and D. Novak, "Microwave photonics combines two worlds," Nat. Photonics **1**(6), 319–330 (2007).
2. R. J. Mailloux, *Phased Array Antenna Handbook* (Artech, 1994).
3. H. Zmuda, and E. N. Toughlian, *Photonic Aspects of Modern Radar* (Artech, 1995).
4. D. Dolfi, P. Joffre, J. Antoine, J.-P. Huignard, D. Philippet, and P. Granger, "Experimental demonstration of a phased-array antenna optically controlled with phase and time delays," Appl. Opt. **35**(26), 5293–5300 (1996).
5. Y. Liu, J. Yang, and J. Yao, "Continuous true-time-delay beamforming for phased array antenna using a tunable chirped fiber grating delay line," Photon. Technol. Lett. **14**(8), 1172–1174 (2002).
6. R. W. Boyd, and D. J. Gauthier, "'Slow' and 'Fast' light," E. Wolf, ed., *Progress in Optics* (Elsevier, 2002), Vol. **43**, Chap. 6, pp. 497–530.
7. J. Mørk, R. Kjær, M. van der Poel, and K. Yvind, "Slow light in a semiconductor waveguide at gigahertz frequencies," Opt. Express **13**(20), 8136–8145 (2005).
8. H. Su, P. Kondratko, and S. L. Chuang, "Variable optical delay using population oscillation and four-wave-mixing in semiconductor optical amplifiers," Opt. Express **14**(11), 4800–4807 (2006).
9. J. B. Khurgin, and R. S. Tucker, *Slow light: Science and Applications* (CRC Press, 2009).
10. Z. Shi, and R. W. Boyd, "Discretely tunable optical packet delays using channelized slow light," Phys. Rev. A **79**(1), 013805 (2009).
11. P. A. Morton, and J. B. Khurgin, "Microwave Photonic Delay Line With Separate Tuning of the Optical Carrier," Photon. Technol. Lett. **21**(22), 1686–1688 (2009).
12. K. Y. Song, M. Herráez, and L. Thévenaz, "Observation of pulse delaying and advancement in optical fibers using stimulated Brillouin scattering," Opt. Express **13**(1), 82–88 (2005).
13. J. Sancho, S. Chin, M. Sagues, A. Loayssa, J. Lloret, I. Gausulla, S. Sles, L. Thevenaz, and J. Capmany, "Dynamic Microwave Photonic Filter using Separate Carrier Tuning based on Stimulated Brillouin scattering in Fibers," Photon. Technol. Lett. in press.
14. L. Thévenaz, "Slow and fast light in optical fibers," Nat. Photonics **2**(8), 474–481 (2008).
15. M. Nikles, L. Thévenaz, and P. A. Robert, "Brillouin gain spectrum characterization in single mode optical fibers," J. Lightwave Technol. **15**(10), 1842–1851 (1997).
16. A. Loaysa, and F. J. Lahoz, "Broad-band RF photonic phase shifter based on stimulated Brillouin scattering and single-sideband modulation," Photon. Technol. Lett. **18**(1), 208–210 (2006).

#133305 - $15.00 USD Received 13 Aug 2010; revised 27 Sep 2010; accepted 28 Sep 2010; published 8 Oct 2010
(C) 2010 OSA

17. M. González Herráez, K. Y. Song, and L. Thévenaz, "Arbitrary-bandwidth Brillouin slow light in optical fibers," Opt. Express **14**(4), 1395–1400 (2006).
18. W. Xue, S. Sales, J. Mork, and J. Capmany, "Widely Tunable Microwave Photonic Notch Filter Based on Slow and Fast Light Effects," Photon. Technol. Lett. **21**(3), 167–169 (2009).
19. M. Sagues, R. García Olcina, A. Loayssa, S. Sales, and J. Capmany, "Multi-tap complex-coefficient incoherent microwave photonic filters based on optical single-sideband modulation and narrow band optical filtering," Opt. Express **16**(1), 295–303 (2008).

1. Introduction

The development of dynamic photonic delay lines is of major importance for broadband digital and analogue signal processing in communication systems. In particular, optical delay lines are extensively studied for microwave systems such as phased array antennas (PAA), microwave photonic filters (MPF) and arbitrary waveform generators, due to their inherent advantages such as large bandwidth, capability of operation over entire RF frequency with low loss and high delay time-signal bandwidth product [1]. In a broadband PAA, the signal bandwidth reaches typically 10-30% of the microwave central frequency. In the classical phase steering scheme, the far-field pattern of the antenna is altered when the microwave frequency is scanned over such a wide range [2,3]. True-time delay (TTD) networks have thus to be introduced. Similarly, most MPFs rely on discrete-time signal processing using real valued coefficients, which requires the use of tunable optical true time delays.

Among the wide diversity of optical delay line schemes that have been reported over the last few years [4–9], slow and fast light (SFL) has been devised as one potential approach to generate continuously tunable signal delays. However, the apparent perfect true time delay generated by slow light suffers from two major obstacles: nearly finite delay time-signal bandwidth product and strictly limited operating frequency. It means that only modest maximal time delay can be expected at high RF frequencies and the operating frequency is essentially limited by the bandwidth of the induced optical resonance, which prevent its complete implementations for practical applications in microwave photonics.

To overcome these limitations, channelized slow light was theoretically studied to increase the maximal achievable delay for broadband digital signals [10]. But, its configuration is considerably complicated and essentially, it suffers from strict phase matching issues between channels. Recently, a new technique, named separate carrier tuning (SCT), was proposed and theoretically investigated. This architecture predicts that significant improvement for the generation of true time delay can be achieved by separately performing photonic microwave phase shifter and slow light in microresonators [11]. The reported TTD of 200 ps limits the applicability of the microresonators approach to high frequency antennas (typically higher than 50 GHz). However, numerous radar systems have a low operating frequency (down to few GHz for ground-based radars) and therefore require up to 10 ns of TTD. It is known that stimulated Brillouin scattering (SBS) gain resonance induces a dispersion, which corresponds to delays up to few tens of ns, but over a limited bandwidth [12]. SBS is therefore a good candidate for SCT technique when few ns of TTD are targeted. In a previous paper [13], we have experimentally verified the validity of the SCT approach transposed to a SBS delay line, using a fiber Bragg grating for optical carrier phase shifting, in a reconfigurable MPF. In this paper, we present a continuously tunable TTD line, in which both phase compensator and slow light systems are controlled by only stimulated Brillouin scattering in optical fibers. In this configuration, we could readily achieve 2π phase shift in gain or even transparent regimes, so that the amplitude variation of RF output signal accompanied with phase shift could be significantly reduced. Also, the required phase shift could be more precisely adjustable in a continuous manner. A complete analysis of the performances of this tunable TTD line is presented for the development of phased array antenna systems and dynamic microwave photonic filters. In addition, the high flexibility of the system is discussed, in terms of operating frequency and signal bandwidth.

#133305 - $15.00 USD Received 13 Aug 2010; revised 27 Sep 2010; accepted 28 Sep 2010; published 8 Oct 2010
(C) 2010 OSA

2. Principle

A key to exert an optical control on the group velocity of light signals, namely slow and fast light is the presence of strong dispersion in materials, which can be readily induced by one or multiple complex optical resonances. The process of stimulated Brillouin scattering in optical fibers is the most widely used mechanism to generate spectral resonances since SBS has shown an unprecedented flexibility of spectral tailoring and large potential bandwidth and room-temperature operation at any desired wavelength [14]. SBS is usually described as nonlinear interaction between two counter-propagating optical waves (a strong pump at v_{pump} and a weak probe wave at v_{probe}), mediated through an acoustic wave. For a particular spectral spacing between two waves ($v_B = v_{pump} - v_{probe}$), fraction of pump light is scattered off into the probe, so that the global effect of the SBS process manifests through a generation of narrow-band gain resonance around $v_{pump} - v_B$, resulting in an exponential growth for the probe wave.

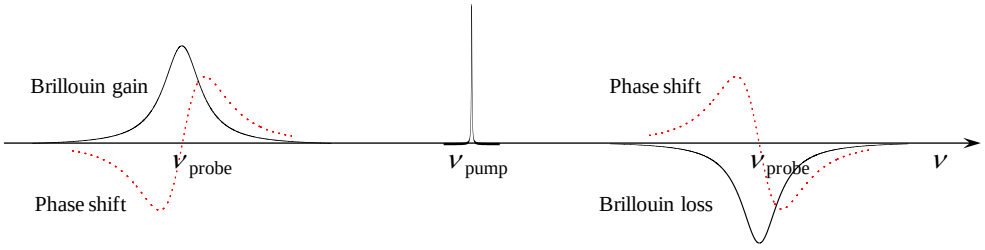

Fig. 1. Brillouin gain and loss resonances and the associated optical phase shifts due to strong dispersion appearing around the resonance.

On the contrary, the energy transfer from the pump to the probe can be assimilated to the generation of a loss resonance as far as the pump wave is concerned. So, by simply swapping the spectral positions of pump and probe, the pump will lead to a spectral absorption centered at the probe frequency $v_{pump} + v_B$. Moreover, it is interesting to discuss that a linear transition of phase shift is associated to the SBS process, in the vicinity of gain/loss resonances, as shown in Fig. 1. In general, true time delay (TTD) is simply achieved by setting the optical carrier frequency in the center of the resonances, leading to a constant group delay and linear phase shift with respect to the microwave frequency. However, in principle, this configuration shows a critical limitation because the true time delay generated by the resonance-induced dispersion only applies within the linear zone of the phase shift, which limits the microwave signal frequency to the resonance bandwidth.

Let us now consider a single sideband modulated optical signal comprising an optical carrier at frequency v_C and a modulation sideband at frequency $v_C + v_{RF}$. A first spectrally broadened Brillouin pump induces a broadband resonance centered at $v_C + v_{RF}$. The signal group delay is then given by the slope of the optical phase at $v_C + v_{RF}$:

$$T_S = \frac{1}{2\pi}\frac{\partial\phi}{\partial\nu}\bigg|_{\nu_C+\upsilon_{RF}}. \tag{1}$$

In broadband applications, the RF signal has a finite bandwidth Δv_{RF} of typically 10-30% of the operating RF frequency v_{RF}. TTD operation implies a constant group delay over the entire frequency range including the carrier and the modulation sideband. Since no information is conveyed in a major part of the large spectral range between the carrier frequency and the modulation sideband centered on the RF signal, TTD operation is simply achieved by calculating the phase shift necessary to make signal and RF group delays match, deduced through the simple expression [11]:

$$T_{RF} = \frac{\phi(\nu_C+\nu_{RF})-\phi(\nu_C)}{2\pi\nu_{RF}} = -\frac{\phi(\nu_C)}{2\pi\nu_{RF}}, \tag{2}$$

#133305 - $15.00 USD Received 13 Aug 2010; revised 27 Sep 2010; accepted 28 Sep 2010; published 8 Oct 2010
(C) 2010 OSA

since the phase shift at the center of the Brillouin resonance $\varphi(\nu_C + \nu_{RF})$ is zero. This situation can be effectively realized by separately managing the dispersion properties at the carrier frequency and around the signal bandwidth, as shown in Fig. 2.

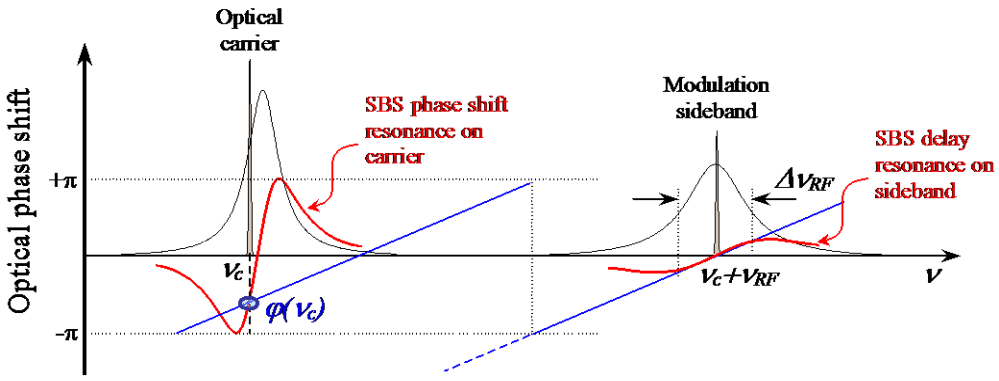

Fig. 2. Principle to correctly operate true time delay over the RF signal bandwidth $\Delta\nu_{RF}$ simply by controlling dispersion properties, separately at carrier frequency and signal bandwidth. ν_C; optical carrier frequency, $\varphi(\nu_C)$; optical phase shift introduced to the optical carrier, ν_{RF}; RF signal microwave frequency.

In our system, a second Brillouin pump generates a narrow-band resonance in the vicinity of the carrier frequency. The phase of the optical carrier is then adjusted to ensure $T_{RF} = T_S$, by simply detuning the central frequency of the resonance with respect to the carrier frequency. As a result, it makes possible to generate correct true time delay for the whole signal bandwidth while dispersion across the entire bandwidth is no longer required unlike typical slow light systems. Also, it must be pointed out that since this optical phase shift is imparted on the carrier, the corresponding phase shift of the electrical signal is therefore constant with respect to the RF frequency. As a consequence, the adjustment of the optical carrier phase $\varphi(\nu_C)$ can be performed modulus 2π. A 360° tunability of the optical carrier is then sufficient to achieve TTD operation. Within the RF bandwidth of interest, this type of TTD generation is conceptually similar to a slow light-based TTD with a dispersion induced by a single broadband resonance centered on ν_C, with FWHM bandwidth of $2\nu_{RF}$. Yet, this new architecture shows two crucial advantages: first, it is independent on the operating RF frequency since the optical resonance can be flexibly displaced at any desired RF frequency; second, it can produce a large TTD with a proper bandwidth at high frequency RF signals since the signal bandwidth of interest is substantially lower than the RF signal frequency.

3. Experimental layout

The schematic diagram of our experimental setup is depicted in Fig. 3, in which two distinct Brillouin slow light systems are basically combined. A 20-km-long dispersion shifted fiber (DSF) was used as a Brillouin gain medium and the Brillouin characteristics of this fiber were measured, showing a Brillouin shift ν_B of 10.73 GHz and an SBS gain bandwidth $\Delta\nu_B$ of 27 MHz. A commercial distributed feedback (DFB) laser diode operating at 1551 nm was utilized as a light source to generate the optical carrier for the microwave signal and two Brillouin pumps using a set of wideband electro-optic modulators (EOM). This way we can obtain high security of stability on spectral distances between the signal and the two Brillouin pumps [15]. The output light was split into two, using an optical coupler. On the signal branch, the light is externally modulated around the operating frequency ν_{RF} (set at 6 GHz) using an electro-optic modulator (EOM) driven by the vector network analyzer (VNA) RF output. The higher frequency sideband was selected by using a fiber Bragg grating (FBG) notch filter. Hereafter this sideband is called RF subcarrier. So, the optical spectrum at the output of the notch filter contains two monochromatic lines, at the carrier frequency ν_C, and at

#133305 - $15.00 USD Received 13 Aug 2010; revised 27 Sep 2010; accepted 28 Sep 2010; published 8 Oct 2010
(C) 2010 OSA

a frequency around v_C + 6 GHz. Then this single sideband modulated signal was delivered into the DSF.

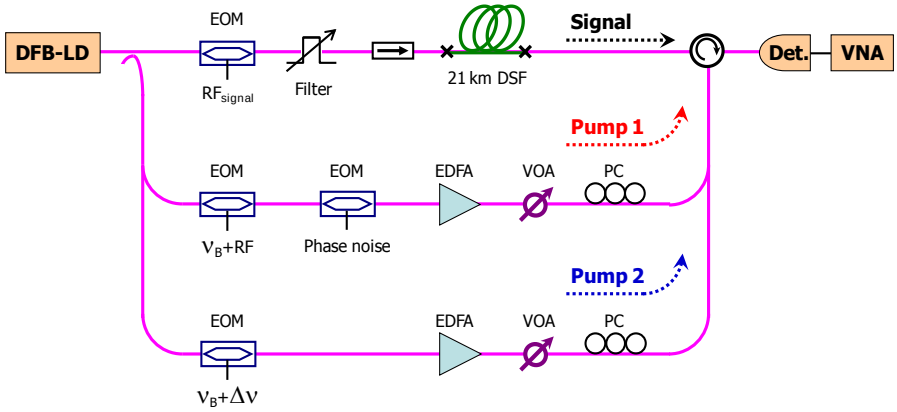

Fig. 3. Schematic diagram of the generation of tunable true time delay, based on separate carrier tuning method. EOM; electro-optic modulator, DSF; dispersion shifted fiber, PC; polarization controller, EDFA; erbium doped fiber amplifier, VOA; variable optical attenuator, VNA; vector network analyzer.

The other branch was also split by two for the generation of two separate Brillouin pumps at different frequencies. The first branch was modulated at $v_B + v_{RF}$ using an EOM driven by an RF synthesizer, and the carrier was completely suppressed by applying an adequate bias to the EOM. Only the higher frequency sideband was selected using a FBG to be used as Pump 1 and then strongly boosted using an erbium doped fiber amplifier (EDFA) to generate strong dispersion around RF subcarrier, thus producing sufficient group delays for microwave signals. The optical power of Pump 1 was controlled using a variable optical attenuator to precisely adjust the amount of group delay. Moreover, its state of polarization was controlled to match the state of signal polarization before entering into the DSF, so as to maximize the Brillouin interaction. Actually, the optical phase of Pump 1 was externally modulated through an external electro-optic phase modulator in order to broaden its power spectrum. So, the spectral width of Pump 1 in the output of the modulator was simply extended by increasing the amplitude of white noise applied to the phase modulator. The maximal bandwidth of Brillouin resonance we obtained in this experiment (hence, instantaneous signal bandwidth) was 100 MHz, as shown in Fig. 4: it was limited in our set-up due to instrumental issues in terms of available power and bandwidth of the white noise. The amplitude variation of the RF signal was measured while the RF subcarrier frequency was swept in the vicinity of the Brillouin resonance induced by Pump 1, representing the spectral profile of the resonance.

The light from the second branch was also modulated through an EOM, at the RF frequency $v_B + \delta v$, and the carrier was fully suppressed following the same scheme. The higher and lower frequency sidebands led to Brillouin gain and loss resonances, respectively, shifted by $+\delta v$ and $-\delta v$ with respect to the carrier frequency, with nearly identical depth and spectral shape. Therefore, the amplitude of the carrier remains almost constant since the gain and loss for the carrier is mutually canceled out, while the associated optical phase shift imparted on the carrier is doubled [16]. The carrier to the resonance frequency detuning δv was then accurately adjusted, within a 15 MHz span, so as to induce the proper phase shift to obtain TTD corresponding to the dispersion slope around RF signal, induced by Pump 1 and applied to the RF signal, as described in section 2.

#133305 - $15.00 USD Received 13 Aug 2010; revised 27 Sep 2010; accepted 28 Sep 2010; published 8 Oct 2010
(C) 2010 OSA

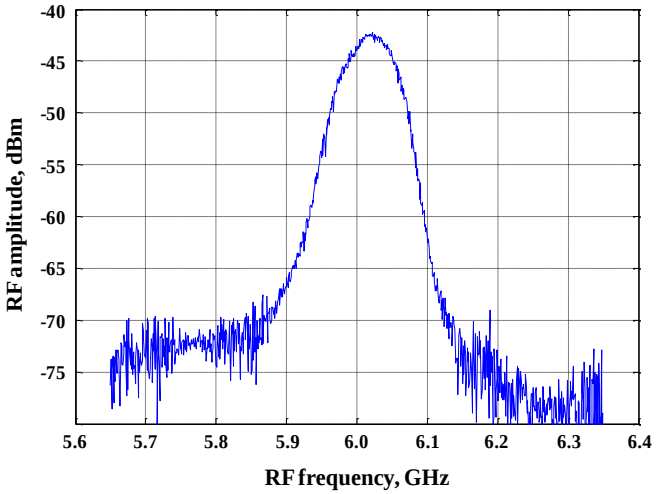

Fig. 4. Variation of the amplitude of RF signal as a function of RF frequency, representing the spectral profile of the effective Brillouin gain resonance induced by Pump 1.

4. Application to phased array antennas and microwave photonic filter

4.1 General implementation

We applied the TTD concepts described in section 2 and 3 for two major microwave photonics applications, namely TTD optically fed phased array antennas and reconfigurable microwave photonic filter. As illustrated in Fig. 5, these two applications are conceptually very close. Indeed, in both systems, an input RF signal $S_i(t)$ is conveyed by the optical carrier and the composite signal is fed to a photonic circuit that first samples the signal in the time

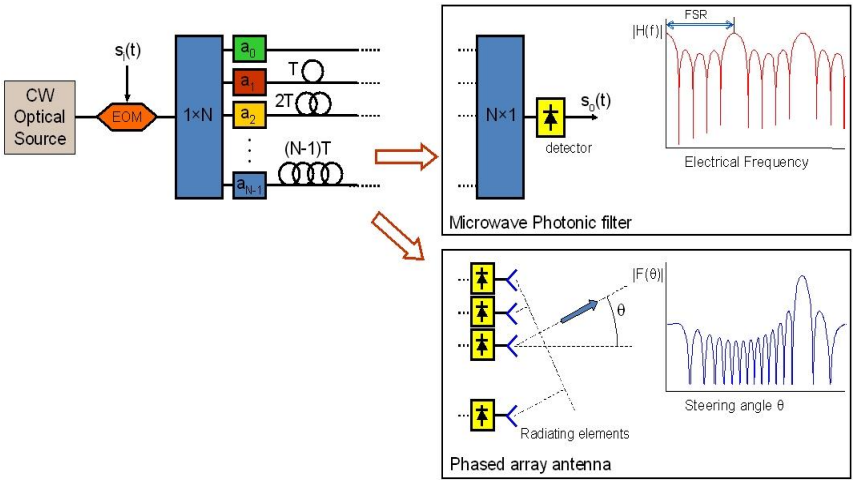

Fig. 5. Layout and transfer functions of generic microwave photonic filters and optically-fed phased array antenna.

domain, using a 1 × N optical coupler and an optical delay lines network, with the delay of the k^{th} line being k × *T*, where *T* is referred to the incremental delay *T*. The sampled signals are

#133305 - $15.00 USD Received 13 Aug 2010; revised 27 Sep 2010; accepted 28 Sep 2010; published 8 Oct 2010
(C) 2010 OSA

then weighted in phase and amplitude to provide the desired filter impulse response, or antenna far field pattern.

In the case of MWP filter, the samples are recombined and RF converted by means of an optical receiver producing the output RF signal $S_0(t)$. The standard electrical/optical impulse response of the optical processor is represented by an equal time spaced (T) pulse train where pulses implement the filter taps. The electrical frequency response of such structure is given by [1]:

$$H(f)=\sum_{r=0}^{N} a_r e^{-i(2\pi r\nu T)}, \tag{3}$$

where ν is the signal RF frequency and a_r are the filter complex coefficients, which are implemented by optical components. In particular, these coefficients determine the extinction ratio of a microwave photonics notch filter. The expression above identifies a transfer function with a periodic spectral characteristic and its frequency period is referred to as the filter free spectral range (FSR). The FSR is essentially inversely proportional to the time spacing between adjacent samples in the impulse response (FSR = 1/T). So, dynamic control of T is basically required for the development of dynamically reconfigurable MPF, providing the tunability of FSR of the filter. MPF is usually performed in incoherent regime, in which the coherence length of the used optical source is shorter than T, since any possible optical interference caused by environmental condition such as temperature and mechanical variation can influence the filter impulse response.

In the case of optically-fed phased array antenna employing TTD networks, the N delayed samples are RF converted by N photodiodes to feed N radiating elements. The normalized angular far-field pattern of the radiated electric field, or antenna diagram $F(\theta)$, is given by the Fourier transform of the output electric field [2]:

$$F(\theta)=\frac{1}{N}\sum_{r=0}^{N-1} a_r e^{-i2\pi r\nu\left(T-\frac{d}{c}\sin\theta\right)}, \tag{4}$$

where θ is the far field angular coordinate and d is the spacing between adjacent radiating elements. The complex coefficients a_r are in this case typically used for side-lobes reduction in the antenna far-field pattern. From Eq. (4), the direction θ_0 of maximum radiated energy can be adjusted by tuning the incremental true time delay T according to:

$$T=\frac{d}{c}\sin\theta_0. \tag{5}$$

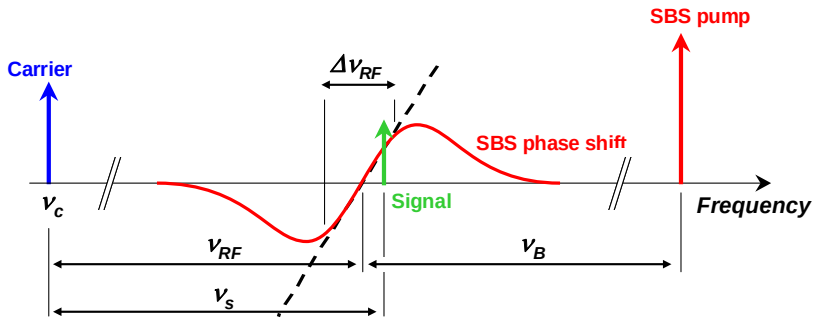

Fig. 6. Schematic diagram of the r[th] elementary single SBS delay line of the phase arrayed antenna.

#133305 - $15.00 USD Received 13 Aug 2010; revised 27 Sep 2010; accepted 28 Sep 2010; published 8 Oct 2010
(C) 2010 OSA

4.2 True Time delay line for optically-fed phased array antennas

From the microwave point of view, the true time delay property refers to the ability of a system to apply a pure and distortion-free delay on input RF signals, independently of the RF frequency. An input signal $S_{in}(t)$ then becomes $S_{out}(t) = S_{in}(t-\tau)$ at the output of the TTD element. In the frequency domain, this is equivalently formulated as:

$$S_{out}(\nu) = S_{in}(\nu) \times e^{-i2\pi\nu\tau}, \tag{6}$$

The phase shift experienced by a monochromatic RF signal through a TTD element is therefore not only linearly dependant but actually proportional to the RF frequency. To avoid the beam squint in an optically-fed phased array antennas, i.e. to ensure that the direction θ_0 of maximum radiated energy does not vary with the frequency ν, the phase transfer functions $\varphi_r(\nu)$ of the r delay lines of Fig. 5 have to obey [2]:

$$\phi_{r+1}(\nu) - \phi_r(\nu) = 2\pi\nu\frac{d}{c}\sin\theta_0 \;\Leftrightarrow\; \phi_r(\nu) = 2\pi r\nu\frac{d}{c}\sin\theta_0 + \phi_0. \tag{7}$$

We now consider an antenna optical feed system using SBS delay lines with only the first Brillouin pump, Pump 1 in section 2, whose gain is centered at $\nu_C + \nu_{RF}$, where ν_C is the optical carrier frequency and ν_{RF} is the central operating RF frequency, as shown in Fig. 6. Through the rth delay line, the RF signal at ν_S then experiences a phase shift $\varphi_r(\nu_S)$, which depends linearly on the RF signal frequency in a spectral bandwidth $\Delta\nu_{RF}$ centered on ν_{RF}:

$$\phi_r(\nu_S) = 2\pi(\nu_S - \nu_{RF})\tau_r, \tag{8}$$

where the delay τ_r is defined as:

$$\tau_r = \frac{1}{2\pi}\frac{\partial\phi_r}{\partial\nu_S}\bigg|_{\nu_S = \nu_{RF}}. \tag{9}$$

The phase shift φ_r thus varies linearly with the RF frequency, but with a phase offset $\varphi_{0,r}$, which is not constant and varies with the generated delay according to:

$$\phi_{0,r} = -2\pi\nu_{RF} \times \tau_r \tag{10}$$

To figure out the consequences of such varying phase offsets, we consider an incremental Brillouin delay distribution such as $\tau_r = r \times T$. The corresponding antenna diagram $F(\theta)$ is:

$$F(\theta) = \frac{1}{N}\sum_{r=0}^{N-1} a_r e^{-ir\left(\phi_r - \frac{2\pi\nu_S d}{c}\sin\theta\right)} = \frac{1}{N}\sum_{r=0}^{N-1} a_r e^{-i2\pi r\left(T(\nu_S - \nu_{RF}) - \frac{\nu_S d}{c}\sin\theta\right)}. \tag{11}$$

Then, for a given operating frequency ν_0, the direction θ_0 of maximum radiated energy is:

$$\sin(\theta_0) = \frac{cT}{d}\frac{\nu_S - \nu_{RF}}{\nu_S} = \frac{\nu_S - \nu_{RF}}{\nu_S} \times \sin(\theta_0)\big|_{TTD}, \tag{12}$$

where $\sin(\theta_0)|_{TTD}$ stands for the true time delay situation with a constant phase offset (Eq. (4)). When $\nu_{RF} = 0$, i.e. when the Brillouin gain is centered on the optical carrier, one retrieves the TTD situation. However, the operating frequency ν_{RF} is limited by the SBS bandwidth to few tens of MHz. Otherwise, first, the scanning angle θ_0 will depend on ν_S (beam squint) and second, when compared to a true time delay system, typically hundred times larger delays will be required to provide the same steering angle θ_0. Indeed, ν_{RF} is typically in the few GHz range and $\nu_{RF} - \nu_S$ in the few tens of MHz range (limited by SBS bandwidth).

As described in section 2, the separate carrier tuning (SCT) technique avoids these problems. Indeed, by tuning the phase of the optical carrier, using here an additional Brillouin system, the phase of the complex coefficients a_r in Eq. (11) can be adjusted to compensate for

#133305 - $15.00 USD Received 13 Aug 2010; revised 27 Sep 2010; accepted 28 Sep 2010; published 8 Oct 2010
(C) 2010 OSA

the phase offset variation described by Eq. (10). The resulting antenna diagram is thus finally given by the TTD expression of Eq. (4).

Fig. 7. Schematic setup of an elementary SCT-SBS true time delay line.

4.2.1 Experimental results

According to the setup in Fig. 7 (see a more detailed description in section 3), we implemented an elementary SBS delay line based on separate carrier tuning technique. The DFB laser emitting at 1551 nm is externally modulated by an electro-optic modulator, driven by the RF signal to be delayed. After detection, the output RF signal phase transfer function is measured using a vector network analyzer (VNA). As described in section 2, the SCT setup basically consists in two Brillouin systems: a SBS-based phase shifter [16], which is responsible for tuning the carrier phase shift; a SBS-based delay line, which controls the microwave subcarrier delay by changing the SBS pump power. According to the above discussion, the electrical phase transfer function of the SCT setup is:

$$H(\nu) = e^{-i\phi_c} \times e^{-i\left(2\pi\nu\tau + \phi_{offset}(\tau)\right)}, \qquad (13)$$

where φ_c is the carrier phase shift, τ is the generated RF signal delay, and φ_{offset} the associated phase offset, described in Eq. (10).

Figure 8(a) shows the phase of the detected RF signal as a function of the RF frequency while the optical carrier phase shift is tuned using the SBS-based phase shifter. The pump power of the SBS delay line is fixed, corresponding to a 10 ns delay. 2π phase tunability is obtained, which is an essential requirement to compensate any value of φ_{offset}. On another hand, Fig. 8(b) shows a similar measurement for a fixed optical carrier phase shift while the pump power of the SBS delay line is varied. The SBS gain spectrum is centered at 6.02 GHz above the optical carrier frequency. For each pump power, the measured phase shift exhibits a linear variation with respect to the RF frequency from 5.955 GHz to 6.075 GHz, showing a bandwidth of 100 MHz. Within this bandwidth, the delay as defined by Eq. (9)

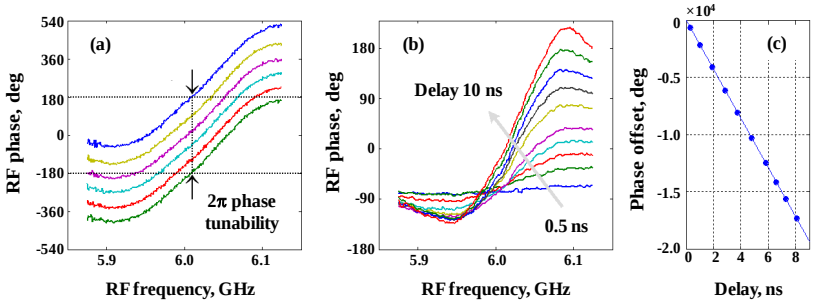

Fig. 8. (a) Fixed RF signal delay, and tuning of the optical carrier phase shift: 2π phase tunability is achieved. (b) Fixed optical carrier phase shift and tuning of the RF signal delay from 0.5 to 10 ns and (c) associated phase offset as a function of the delay.

#133305 - $15.00 USD Received 13 Aug 2010; revised 27 Sep 2010; accepted 28 Sep 2010; published 8 Oct 2010
(C) 2010 OSA

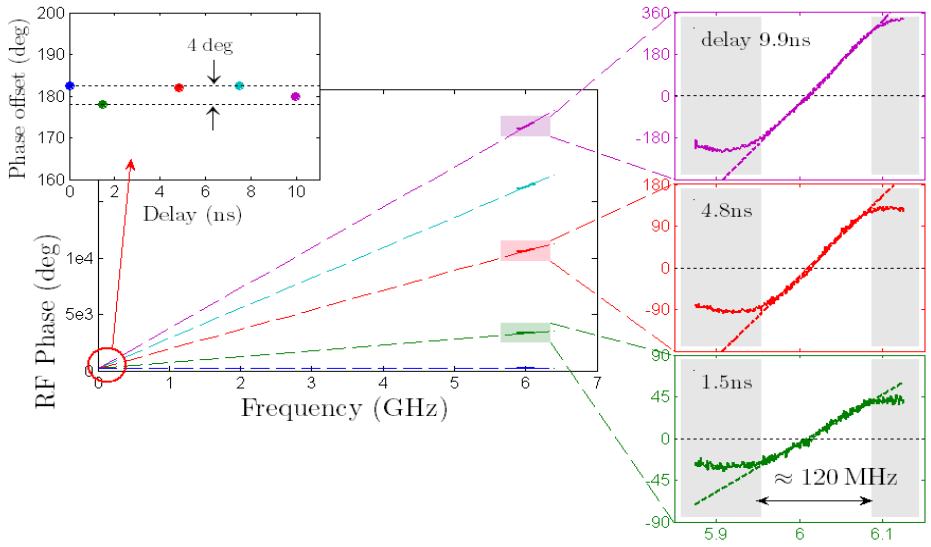

Fig. 9. SBS-SCT based true-time delay line. For delays from 0.03 to 9.9 ns, the optical carrier phase shift is adjusted to ensure a constant extrapolated phase offset at the origin of RF frequencies (top inset). A 100 MHz instantaneous bandwidth is obtained.

varies from 0.5 to 10 ns while the SBS pump power is increased. Figure 8(c) shows the phase offset as a function of the applied delay corresponding to Fig. 8(b) data. For true time delay operation, the optical carrier phase shift has then to be adjusted for each delay in order to finally obtain a constant phase offset with respect to the delay.

Figure 9 shows the experimental validation of this concept for delays of 0.03, 1.5, 4.8, 7.5 and 9.9 ns. On the central figure, we plotted the measured phases plus an integer number n times 2π, where n is defined as:

$$\phi_{offset}(\tau) = \mathrm{mod}\left(\phi_{offset}(\tau)\right) - n \times 2\pi, \tag{14}$$

where *mod* is the modulus 2π function. The RF phase curves are plotted versus the RF frequency, and the linear regions of the phase curves have been extrapolated down to the origin of frequencies. The right insets show zooms of the phase measurements within the Brillouin spectral bandwidth for delays of 1.5, 4.8 and 9.9 ns. On the top inset, we plotted the residual phase offset after compensation by the SBS-based phase shifter. For all delays, the phase offset is equal to 180° ± 2°. The SCT delay line therefore operates as a TTD element, providing a tuneable TTD up to 10 ns, within an instantaneous RF bandwidth of 100 MHz. The operating frequency of 6 GHz was in our case limited by equipment availability, but the SBS-based SCT technique can be in principle applied at any operating frequency.

4.2.3 Antenna performances extrapolation and discussion

We consider a typical phased array antenna with 32 × 32 radiating elements and operating at the central frequency ν_{RF}. The spacing between adjacent elements d is half of the microwave period. The maximum required true-time delay τ_{max} for a ± 45° scanning is then 15 microwave periods, which is $15/\nu_{RF}$ [4]. Most radars operate between 2 and 20 GHz, which corresponds to maximum required delays, typically ranged from 1 to 10 ns. In the SBS-SCT system described above, we obtained a maximum delay of 10 ns for a Brillouin pump power of 110 mW with a spectral broadening of the pump that gives an instantaneous bandwidth $\Delta\nu_{RF}$ of 100 MHz. By further broadening the pump spectrum, $\Delta\nu$ can be enlarged, but the maximum delay will decrease accordingly, with $\Delta\nu_{RF} \times \tau_{max}$ approximately constant [17]. As a result, in

#133305 - $15.00 USD Received 13 Aug 2010; revised 27 Sep 2010; accepted 28 Sep 2010; published 8 Oct 2010
(C) 2010 OSA

an optimized setup, in which the pump spectrum has been broadened to its maximum, but still providing $\tau_{max} = 15/\nu_{RF}$, one has:

$$\Delta\nu_{RF} \times \frac{15}{\nu_{RF}} = 10\,ns \times 120\,MHz \quad \Leftrightarrow \quad \frac{\Delta\nu_{RF}}{\nu_{RF}} = 8\%. \tag{15}$$

The relative instantaneous bandwidth $\Delta\nu_{RF}/\nu_{RF}$ of the optimized system therefore does not depend on the operating frequency and remains 8%. It can eventually be further increased using higher pump powers for broadband radar applications, in which $\Delta\nu_{RF}/\nu_{RF}$ of 10-20% is required. Figure 10 represents the simulated antenna diagrams for an optically-fed phased array antenna comprising 32 × 32 SCT-based SBS delay lines as described in section 4.2.2. The operating frequency is 6.025 GHz and the signal bandwidth is 8%, according to Eq. (15). The maximum delay required for ± 45° scanning is calculated as 2.5 ns.

Figure 10(a) illustrates the situation that only SBS optical carrier phase shift is performed. The phase shift between adjacent radiating elements is then constant versus microwave frequency. It results in a detrimental variation of the scanning direction within the RF signal bandwidth (beam squint) [2]. On another hand, Fig. 10(b) shows the case, in which the SBS delay is solely applied using the SBS gain centered on the microwave subcarrier. In this case, each delay line actually produces a phase shift linearly dependent on the RF frequency according to Eqs. (8) to (12), but with a phase offset that varies from one delay line to another one. As a consequence, the scanning angle is reduced close to zero (see Eq. (12)), and also a critical beam squint is observed. Finally, Fig. 10(c) shows the SCT technique, in which the same incremental delays as shown in Fig. 10(b) are produced by the Brillouin gain centered on the microwave subcarrier, but the phase offsets are compensated by the optical carrier phase shifting. This configuration leads to a beam squint-free antenna diagram, so all RF frequency components compounding of the signal are steered in the same direction. The ± 2° fluctuation of the phase offset observed in our experiment was taken into account in our simulation as a random offset distribution. However, it is clearly seen that it does not generate any critical increase of side lobes, when compared to an ideal TTD system.

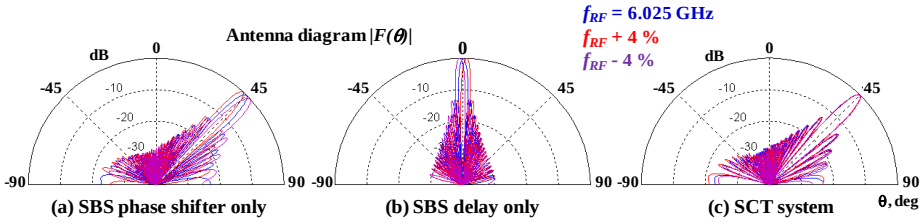

Fig. 10. Simulated antenna diagrams for 32 × 32 radiating elements and SBS based delay lines. (a): Use of SBS optical carrier phase shift only; (b): use of SBS delay only; (c) use of separate carrier tuning technique for true time delay lines. The RF frequency ν_{RF} is 6.025 GHz (in blue), ν_{RF} + *5%* (in red), and ν_{RF}-*5%* (in magenta.

4.3 Microwave photonic filter

In a multi-tap complex coefficient filter, the separate carrier tuning technique enables to independently adjust the elementary delay T between adjacent filter branches, and the phase of the complex coefficients a_r. Then, as T becomes αT, a homothetic transformation of the filter spectral response is obtained, corresponding to a FSR change:

$$H'(\nu) = \sum_{r=0}^{N-1} a_r e^{-2i\pi r(\alpha\nu)T} = H(\alpha\nu). \tag{16}$$

On another hand, when the complex coefficients are changed by shifting the optical carrier phase by $\varphi(\nu_C)$:

#133305 - $15.00 USD Received 13 Aug 2010; revised 27 Sep 2010; accepted 28 Sep 2010; published 8 Oct 2010
(C) 2010 OSA

$$a_r \rightarrow a_r \times e^{ir\phi(\nu_C)}, \tag{17}$$

then the filter response is translated in the frequency domain by $\varphi_0/(2\pi T)$:

$$H'(\nu) = \sum_{r=0}^{N-1} a_r e^{ir\phi(\nu_C)} e^{-2i\pi r\nu T} = \sum_{r=0}^{N-1} a_r e^{-2i\pi r\left(\nu - \frac{\phi(\nu_C)}{2\pi T}\right)T} = H\left(\nu - \frac{\phi(\nu_C)}{2\pi T}\right). \tag{18}$$

The filter is then fully reconfigurable: its FSR can be changed (Eq. (16)), and the spectral origin of the FSR change can be adjusted (Eq. (18)).

4.3.1 Filter implementation

Figure 5 depicts the basic configuration of notch-type incoherent microwave photonic filter, which yields a periodic notch response. The experimental setup of SBS-based tunable MPF is illustrated in Fig. 11. We used two distinct DFB lasers, which are mutually incoherent. So, the minimal time delay *T* in the filter is naturally not limited by the coherence length of the laser, hence it makes possible to obtain a higher FSR for the filter. Furthermore, the spectral distance between two lasers were properly adjusted at 150 GHz, so that we can avoid any signal distortion, possibly caused by the beating frequency between two lasers. Light outputs from the two lasers were fed to an EOM and modulated at desired RF frequency, which is subject to be filtered. They propagated through differential optical path and only one signal was delivered to the tunable true time delay system, based on stimulated Brillouin scattering as previously described in Section 3. Then they were recombined to mutually interfere and the amplitude and phase of RF signal was monitored by a vector network analyzer to analyze characteristics of the RF filter transfer function.

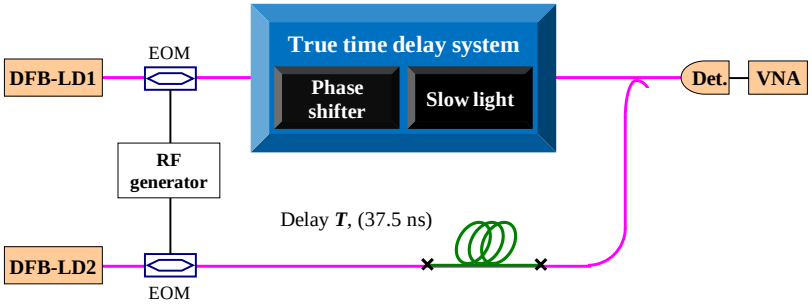

Fig. 11. Experimental layout of dynamically reconfigurable microwave photonic filter, based on stimulated Brillouin scattering in fibers.

4.3.2 Experimental results

The RF subcarrier frequency was swept in the vicinity of the Brillouin resonance and the amplitude and phase RF signal after propagating through the Brillouin gain medium was measured as a function of RF frequency, as shown in Fig. 12. It is clearly observed that the microwave phase has a linear dependence on shift as a function of RF frequency, with a bandwidth of 100 MHz and moderate amplitude change of 4 dB. The corresponding phase shift of the microwave signal with respect to the RF frequency within a 100 MHz range is also illustrated. There is a linear phase change and also a moderate change in the Brillouin gain. It is very important for the MPF to control not only the TTD, but also the amplitude coefficients of the filter, i.e. a_1 or a_2. To implement the TTD, a linear phase slope is required. In this case,

#133305 - $15.00 USD Received 13 Aug 2010; revised 27 Sep 2010; accepted 28 Sep 2010; published 8 Oct 2010
(C) 2010 OSA

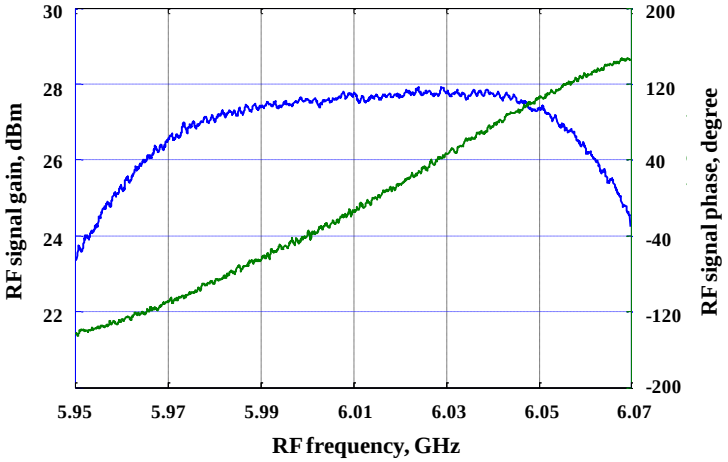

Fig. 12. SBS gain profile within RF signal bandwidth and the associated linear phase shift.

the maximum achievable TTD value over the 100 MHz span is 7 ns. This delay can be tuned by changing the optical power of the Brillouin pump signal.

To check the filter tunability, we first measured the effect of a pure phase shift on the optical carrier by recording the filter spectral transfer function. In this case, it corresponds to a complex-valued two-coefficient MPF [1,18,19]. Figure 13 displays the frequency response of the filter obtained with the SBS pump turned on and thus a fixed TTD, preserving the free spectral range. In this figure, continuous tunability was demonstrated as the phase of the lower-coefficient tap is modified by tuning the carrier phase shift using SBS-based phase shifter. Experimental measurements (symbols) have excellent agreements with theoretical calculations (dashed lines). The observed small deviations of the RF response from the ideal behavior are attributed to the non-completely flat phase response generated by SBS system. It must be considered that a noise source is used to broaden the Brillouin gain, resulting in small deviations from the Gaussian gain shape and thus in phase fluctuations.

It must be pointed out that the central frequency of the notch filter is tuned while maintaining the shape of the transfer function unaltered, since the true time delay between the arms of the MPF is fixed. The maximum achievable phase shift is greater than 360°, which leads to a continuously full tuning range of the filter response. This technique can be implemented to obtain a RF frequency-independent phase shift; in our case, the filter central frequency is practically limited by our instrumentation.

#133305 - $15.00 USD Received 13 Aug 2010; revised 27 Sep 2010; accepted 28 Sep 2010; published 8 Oct 2010
(C) 2010 OSA

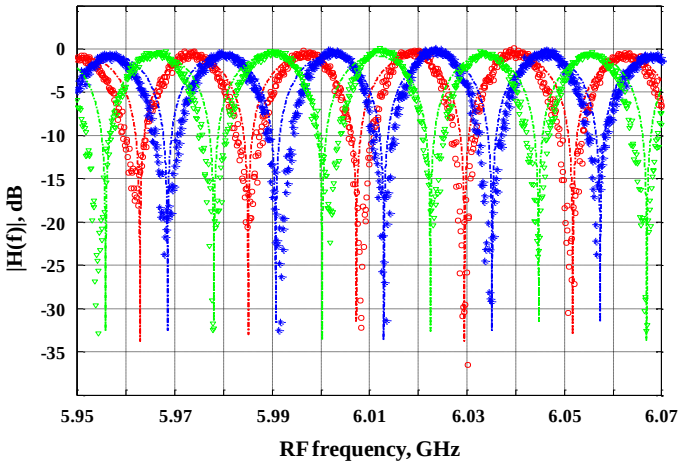

Fig. 13. Measured (symbol) and simulated (dashed line) filter frequency response (a) tuning the carrier phase shift for 110 mW Brillouin pump power.

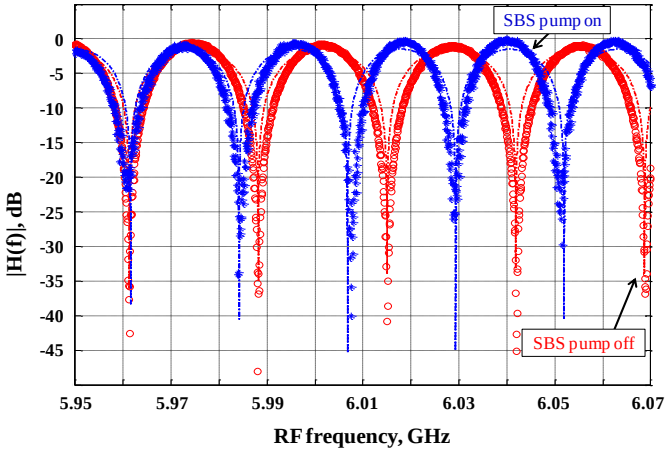

Fig. 14. Measured (symbol) and simulated (dashed line) frequency response of MPF with (red) and without (blue) Brillouin pump power at 110 mW.

To get the tunability of the free spectral range, we implemented a SBS-based tunable delay in one of the branches. The two branches of the MPF have a path imbalance of 7.5 m, corresponding to T_0 = 37.5 ns and resulting in a FSR of 26.7 MHz. TTD can be generated using the SCT technique, which must lead to a different spectral response of the MPF, since its FSR will change upon tuning the delay. Figure 14 confirms that the FSR of the filter changes when the pump is applied. When a 110 mW pump power is launched into the higher branch of the MPF, SBS generated a delay of about 7 ns at 6 GHz with 100 MHz bandwidth. This means that the FSR will be decreased down to 22.5 MHz, which corresponds to a 20% FSR reduction. The SBS-based phase shifter is then used to maintain a notch position at a given frequency. Indeed, according to Eq. (3) and (8), the frequency response of the 2-tap notch filter is given by:

$$H(\nu) = \cos^2\left(\frac{\phi(\nu_c)}{2} - \pi\nu T_0 - \pi(\nu - \nu_{RF})T\right), \tag{19}$$

#133305 - $15.00 USD Received 13 Aug 2010; revised 27 Sep 2010; accepted 28 Sep 2010; published 8 Oct 2010
(C) 2010 OSA

where ν_{RF} is the RF central frequency (6.015 GHz in our case). A notch can then be position at any arbitrary frequency ν_{notch} provided that the optical carrier phase shift $\varphi(\nu_c)$ satisfies:

$$\phi(\nu_c) = \mathrm{mod}\left(\pi + 2\pi\nu_{notch}T_0 + 2\pi T\left(\nu_{notch} - \nu_{RF}\right)\right), \tag{20}$$

where *mod* is the modulus 2π function. In our particular case illustrated in Fig. 14, 302.4° of carrier phase compensation were required to fix a notch position at 5.967 GHz. A reconfigurable notch filter with more than 30 dB extinction ratio has finally been achieved, showing an excellent agreement with theoretical prediction from Eq. (3).

6. Conclusion

In this paper, we experimentally demonstrated that Brillouin slow light elements offer novel and outstanding capabilities in microwave photonics systems, particularly thanks to an innovative all-optical tuneable true-time delay line based on separate carrier tuning technique. We implemented two SBS systems to separately manage the dispersion characteristics at the optical carrier and RF subcarrier frequencies. A TTD continuously tuneable from 0 to 10 ns is achieved, with a 100 MHz instantaneous bandwidth, and at an operating frequency of 6 GHz. However, it must be pointed out that this technique has no physical limitation on operating RF frequency since the Brillouin resonance can be positioned at any desired RF frequency. In addition, Brillouin systems can provide a signal bandwidth up to 12 GHz with high flexibility, which can allow us to operate the system at higher RF frequencies up to 150 GHz as far as 8% relative bandwidth is concerned. By extrapolating the performances of this setup used in a potential phased array antenna feeding system, we showed that SCT technique meets the requirements for ± 45° scanning at any operating frequency and with an instantaneous bandwidth of 8%. Besides, we experimentally demonstrated the implementation of the SBS-based SCT technique in a reconfigurable microwave photonic notch filter operating around 6 GHz. The tunable TTD induced in our setup allowed a 20% tunability of the FSR of the filter, and the optical carrier phase shifting then enabled to control the origin of the FSR variation, matching the reference frequency. Therefore, we believe that this technique can show the high suitability and key role of slow light for microwave photonics applications

Moreover, SCT-SBS true time delay offers simultaneously a continuously tunable time delay and amplitude/phase control while other reported photonic TTD devices provide either continuous delay without amplitude/phase control [5], or discrete delays and phase control [4]. It means that more sophisticated beam forming can be realized with side-lobe reduction and no additional complexity of the system. However, the scalability of this system in terms of required optical power might act as a critical limitation in practical implementations.

Acknowledgements

We acknowledge the support from the Swiss National Science Foundation through project 200020-121860 and the support from the European Union FP7 project GOSPEL.

#133305 - $15.00 USD Received 13 Aug 2010; revised 27 Sep 2010; accepted 28 Sep 2010; published 8 Oct 2010
(C) 2010 OSA